4.5 A NUMERICAL SIMULATION OF AIR FLOWS OVER AN URBAN AREA: VERIFICATION OF AIR FLOWS OVER 2-D AND 3-D OBSTACLES WITH WIND TUNNEL MEASUREMENTS

Tetsuji Yamada*
Yamada Science & Art Corporation

1. Introduction

Considerable interest exists in understanding air flows and dispersion of airborne materials in an urban environment. Urban areas are known to be warmer (urban heat islands) than surrounding rural areas due to anthropogenic heat releases and modifications of soil surfaces by concrete structures. Buildings block air flows, and air flows are accelerated in the building corridors. Urban areas contribute significantly to the modification of microclimate. Urban areas present unique environmental problems. Automobile emission, and accidental and terrorist releases of toxic materials in an urban environment result in a potentially serious consequence due to high population density.

Several approaches were considered to incorporate urban effects into numerical models. One approach is to treat buildings as roughness elements. This method is appropriate only when the interest is limited in the layer above the building height. It is not, however, appropriate if the interest includes air flow on the street level, which is the case discussed here.

A second approach is to treat buildings in a fashion similar to tall tree canopies. Buildings induce drag to the air flows. Building clusters are parameterized in terms of the ratios of building volume to the grid volume. This approach is common in the atmospheric models where the horizontal grid size is too large to resolve each building.

A third approach is to simulate air flows around each building. This approach is ideal and common in the computational fluid dynamics (CFD) community, but computation becomes expensive if the number of buildings in a simulation area is very large.

A typical grid size for a CFD model is 1 m while a typical grid size for an atmospheric model is 1 km. In other words, a difference of three orders of magnitude exists in grid size between a CFD model and an atmospheric model. In addition, CFD models typically provide steady state solutions while atmospheric models deal with diurnal variations. Atmospheric models include water vapor, clouds and precipitation, but CFD models do not. Thus, not only grid size, but also model physics are significantly different between the CFD and atmospheric models.

Recently, there have been some efforts in combining the CFD and atmospheric models capabilities to address effects on air flows from a building to terrain scales. This is what is required to simulate air flows over the urban areas in complex terrain and/or coastal areas. This paper discusses how an atmospheric model was improved to simulate air flows around buildings under the influence of mesoscale wind variations.

2. Model

The governing equations for mean wind, temperature, mixing ratio of water vapor, and turbulence are similar to those used by Yamada and Bunker (1988). Turbulence equations were based on the Level 2.5 Mellor-Yamada second-moment turbulence-closure model (1974, 1982). Five primitive equations were solved for ensemble averaged variables: three wind components, potential temperature, and mixing ratio of water vapor. In addition, two primitive equations were solved for turbulence: one for turbulence kinetic energy and the other for a turbulence length scale (Yamada, 1983).

The hydrostatic equilibrium is a good approximation in the atmosphere. On the other hand, air flows around buildings are not in the hydrostatic equilibrium. Pressure variations are generated by changes in wind speeds, and the resulted pressure gradients subsequently affect wind distributions. We adopted the HSMAC

* *Corresponding author address:* Ted Yamada, Yamada Science & Art Corporation, 13 Heiwa, Santa Fe, NM 87506 USA E-mail: ysa@ysasoft.com www.ysasoft.com

(Highly Simplified Marker and Cell) method (Hirt and Cox, 1972) for pressure computation because the method is simple yet efficient. The method is equivalent to solving a Poisson equation, which is commonly used in non-hydrostatic atmospheric models. We tested both the HSMAC method and solving a Poisson equation, and found that the HSMAC method produced the results that appear to be more realistic.

Boundary conditions for the ensemble and turbulence variables are discussed in detail in Yamada and Bunker (1988). The temperature in the soil layer is obtained by numerically integrating a heat conduction equation. Appropriate boundary conditions for the soil temperature equation are the heat energy balance at the ground and specification of the soil temperature at a certain distance below the surface, where temperature is constant during the integration period. The surface heat energy balance is composed of solar radiation, long-wave radiation, sensitive heat, latent heat, and soil heat fluxes. For steady state simulations, computation of soil temperature is turned off so that temperature does not change with time.

Lateral boundary values for all predicted variables are obtained by integrating the corresponding governing equations, except that variations in the horizontal directions are all neglected. The upper level boundary values are specified and these values are incorporated into the governing equations through a four-dimensional data assimilation method (Kao and Yamada, 1988).

3. Comparison with observation

HOTMAC (Higher Order Turbulence Model for Atmospheric Circulation) was previously applied to simulate air flows in the areas whose horizontal extents were in the order of 10 km (Yamada and Bunker, 1988, 1989) to over 1000 km (Kao and Yamada, 1988). The horizontal grid spacing for those simulations was from several hundred meters to as large as 50 km.

For simulations of urban air flows, horizontal grid spacing must be small enough to resolve separations and re-circulations of air flows around buildings. On the other hand, computations become quite extensive since small grid spacing requires a short integration time step in order to satisfy the criteria for numerical stability.

Quantitative comparison of model results with observations for air flows in an urban area encounters considerable difficulties. Present models cannot include details of urban morphology and observations become prohibitively expensive to obtain representative wind and turbulence distributions in a large city. Although a simulation of air flows in a city is our desirable goal, we are necessitated to test model capabilities under simplified boundary conditions. Preliminary tests indicated horizontal grid spacing of 10 m or less was required to simulate separations and re-circulations of air flows around a building. It was also desirable that horizontal and vertical grid spacing were in the same order of magnitude. A number of iterations to satisfy the convergence criterion increased considerably if the horizontal grid size was significantly larger than the vertical grid spacing. The vertical grid spacing near the surface was in the order of a few meters in order to accurately resolve large gradients of wind and temperature profiles.

3.1. Air flows over two- and three-dimensional hills

Mountains and hills are irregular in shape, and wind and turbulence distributions over topography vary greatly in space and time. These variations make accurate measurements and simulations difficult to obtain. Consequently, it hinders quantitative comparison of model results with observations. To avoid the problems associated with topographic irregularities, air flows over hills and mountains of simplified shapes were studied extensively in laboratory facilities (Hunt and Snyder, 1980; Ishihara et al., 2001). Most wind tunnel experiments were conducted under neutrally stratified conditions, while water channel experiments addressed effects of density stratification on currents and turbulence.

Even with simple geometry such as a cosine shaped hill, wind distributions measured in a wind tunnel were quite complex (Ishihara et al., 2001). Flow separation, re-circulations, and reattachment were observed behind 2-d and 3-d hills. For a 3-d circular hill, a pair of vortices was observed over the slopes of downstream side. The vortices were resulted from a combination of reversed flow and air flows converged behind a circular hill.

Ishihara et al. (2001) found that streamlines of upwind side of 2-d and 3-d hills are similar. However, significant differences were observed in the streamlines downstream of hills. For a 2-d hill, streamlines were closed, while for a 3-d hill, streamlines were not closed. In other words, the streamlines separated at the crest of a 3-d hill did not touch the floor (Figs. 4 and 5 of Ishihara et al., 2001).

We used HOTMAC to reproduce observed streamline behaviors for 2-d and 3-d hills. A Gaussian (normal distribution) shaped circular hill was placed in a computational domain of 730 m x 440 m. The center of hill was located at (250 m, 220 m). The height of a hill was 200 m and the standard deviation of normal distribution was 100 m. Horizontal grid spacing was 5 m and the vertical grid spacing was 4 m near the ground and increased with height. The top of computational domain was 1000 m. The number of grid points was 147 x 89 x 21.

Neutral stratification and steady state boundary conditions were assumed. Computations continued until flow patterns reached approximately steady state. Figure 1a shows streamlines in the x-z vertical cross section along the centerline of the 3-d hill. As pointed out by Ishihara et al. (2001), the flow re-circulation area behind the hill stayed aloft and the streamlines separated at the crest did not reach the ground. Ishihara et al. (2001) called them as “opened streamlines” and distinguished them from “closed streamlines” observed behind a 2-d hill.

HOTMAC uses the UTM (Universal Traverse Mercator) coordinate system, which is a map projection method and often adopted by atmospheric models. The globe is divided into 60 zones in the longitudinal direction. The coordinate at the point where the center meridian of each zone meets the equator is (500 km, 0 km). This is why the x and y coordinates are given in km in some figures in the paper. The vertical coordinate is also given in km since a typical height of computational domain is 5-10 km for atmospheric simulations.

We also conducted simulations over a 2-d hill using the same computational domain as for the 3-d simulation. Boundary conditions at the side boundaries were that *U*s were the same as those along the centerline of the computational domain and *V*s were zero. Figure 1b shows streamlines in the *x-z* cross section along the centerline of the computational domain. The re-circulation area was much larger than the counterpart for a 3-d hill and the streamlines separated at the crest touched the ground. Ishihara et al. (2001) explained why the streamlines for a 3-d hill were opened while those for a 2-d hill were closed. For a 2-d simulation, $\partial V/\partial y=0$ in the mass conservation equation. Thus, the upward motion must be compensated by *U* to satisfy the mass conservation. On the other hand, $\partial V/\partial y\neq 0$ along the centerline of a 3-d hill. Thus, the upward motions were compensated by not only *U* but also *V* to satisfy the mass conservation. In other words, *U* was less disturbed for a 3-d simulation than for a 2-d simulation, which resulted in a smaller and non-closed re-circulation. The present results were in good agreements with those obtained by Ishihara and Hibi (2000) where a *k*-ϵ model was applied.

3.2 Air flows over two- and three-dimensional building arrays

The objective is to simulate air flows around buildings in a city that is located in the area where topographic influence is significant. To do so, the model is required to have the capabilities to simulate air flows both around buildings and over topography. In the previous section, the model demonstrated the capabilities in simulating air flows over 2-d and 3-d steep hills. In this section we will apply HOTMAC to simulate air flows around a single and multiple buildings. Considerable work has been conducted both experimentally and numerically to study air flows around a bluff body such as a cube. An excellent review was given in a book by Murakami (2000).

Brown et al. (2001) measured velocity distributions for two- and three-dimensional building arrays in a wind tunnel. The purpose of the experiments was to provide high-quality and spatially dense data, which are used to evaluate performance of computational fluid dynamics (CFD) models. There were significant differences in the measured wind and turbulence characteristics for the 2D and 3D arrays.

HOTMAC was used to simulate the wind tunnel data. For various reasons, we could not maintain in the model the same boundary conditions as in the experiments. For example, the 2D array in the experiments consisted of 7

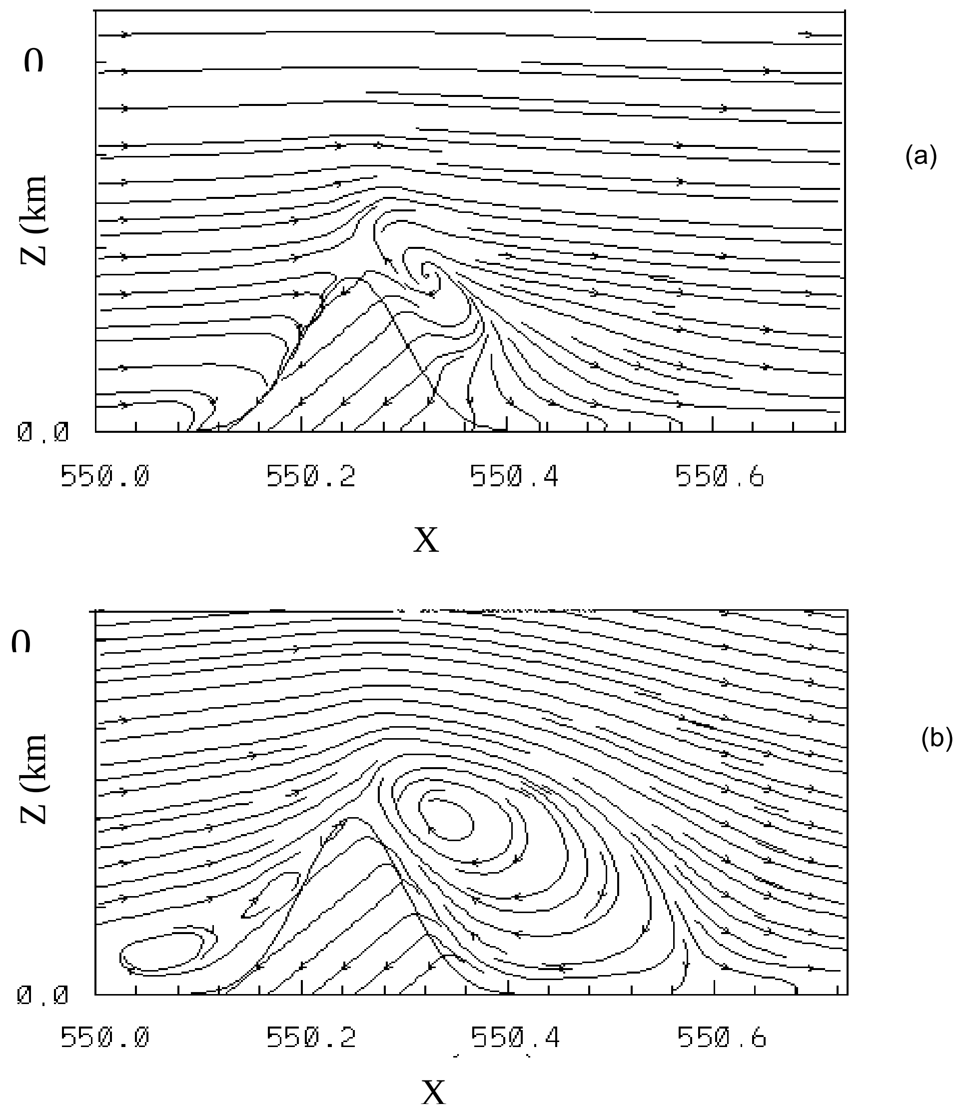

Figure 1: The modeled streamlines in the x-vertical cross section along the centerline of a) a 3-d hill and b) a 2-d hill

rectangular blocks (0.15 x 0.15 x 3.7m) placed with their long faces perpendicular to the flows and with a spacing of one building height (0.15m) between buildings in the along wind direction. However, in the numerical simulations, the 2D array consisted of 3 rectangular blocks (28 x 30 x 200 m) in order to save computational time.

The 3D array in the experiments consisted of 7 x 11 cubes (0.15 x 0.15 x 0.15 m) with one height spacing between cubes. On the other hand, the 3D array in the model simulations consisted of 3 x 3 rectangular buildings (28 x 28 x 30 m) with one height (30 m) spacing between buildings. Although the boundary conditions for the experiment and the model simulations were not identical, many important features observed in the experiments were successfully reproduced in the model results as discussed below.

The purpose of this section is to demonstrate that HOTMAC is capable to simulate qualitatively separations, re-circulations, and reattachment of streamlines observed in the flows around bluff bodies. All bluff body simulations were conducted under neutral stratifications in a domain of 400 m x 200 m x 500 m (vertical). The horizontal grid spacing was 4 m and the vertical gird spacing was 4 m near the ground and increased with height. A total number of grid points were 101 x 51 x 21.

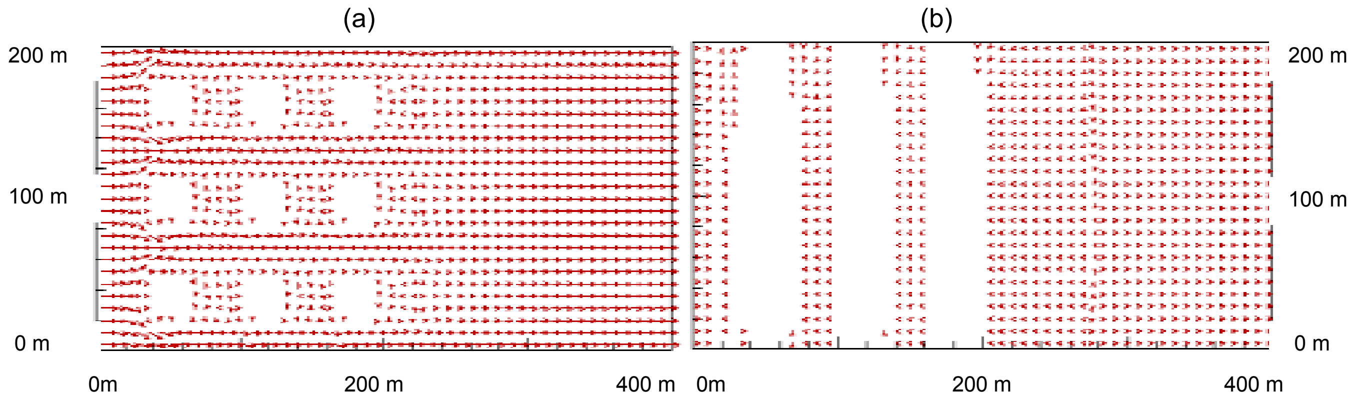

Figure 2: The model shows wind distribution at 10 m above the ground for the a) 3D array, and b) 2D array.

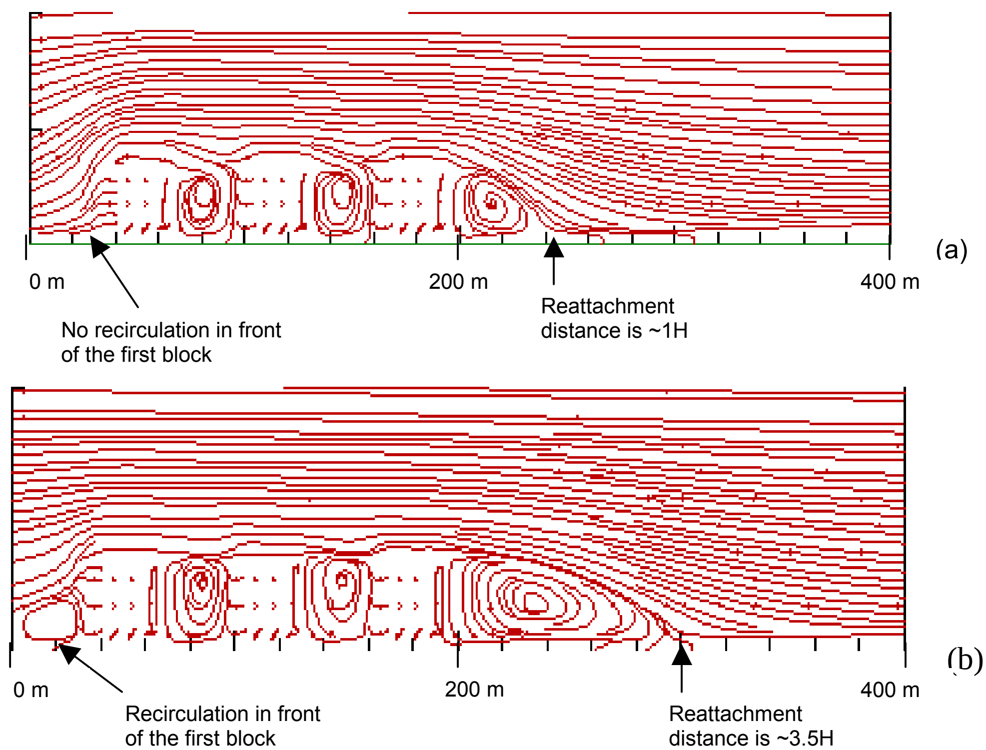

Figure 3: The modeled streamlines in the vertical cross section along a centerline of the a) 3D array, and b) 2D array.

Figure 2a. shows wind distributions at 10 m above the ground for the 3D array. The arrows indicate wind directions and the length of an arrow is proportional to the wind scale, which is shown at the left upper corner of the figure. The approaching winds collided with the building wall, which resulted in increasing dynamic pressure. The pressure gradient created by the collision diverged winds horizontally and vertically. The flows around the upwind corners were accelerated, and the flows behind downwind corners were separated from the building. The flows behind the building and along the centerline were reversed. The reversed flows and main flows formed a pair of symmetric circulations.

Figure 2b shows wind distributions at 10 m above the ground for the 2D array. Flow directions are nearly parallel to the centerline of the computational domain. Flow reversal is evident

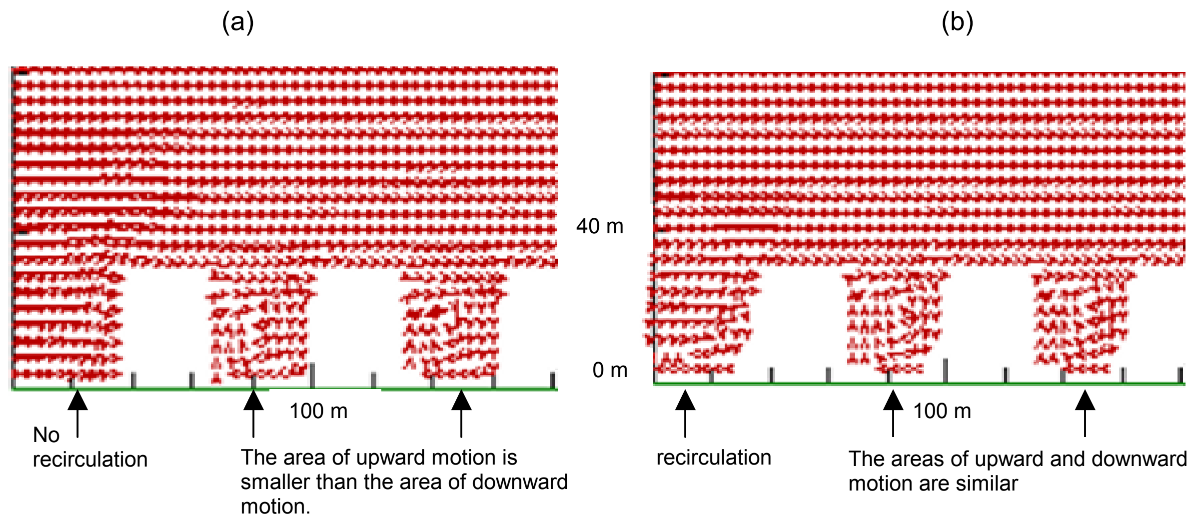

Figure 4: The modeled wind distributions in the vertical cross section along a centerline of the a) 3D array, and b) 2D array.

along the line whose distance is approximately 300 m from the inflow boundary.

Figure 3a shows the streamlines in the *x-z* vertical cross section for the 3D array along the centerline of the buildings. Flow separations, recirculations, and reattachment are clearly indicated. Wind tunnel experiments often show a small re-circulation area at the leading edge of the first building roof. The present simulation also indicated such re-circulation, but it was not as clear as in measurements. The flow reattachment occurred approximately 1 H behind the third building, which was in good agreement with the measurements.

Figure 3b shows the streamline for the 2D array along the centerline of the buildings. Separations, re-circulations, and reattachments are evident. Flows between the buildings change as the distance between the two buildings changes. If the distance is significantly large, interaction between the buildings will diminish. On the other hand, if the distance is small, then the two buildings will act like a single building. The flow reattachment behind the third building is approximately 3.5H, which is over three times of the counterpart for the 3D array. The measurements indicated the reattachment distance was approximately 3.5 H.

Figures 4a and 4b show circulations in front and between the buildings for the 3D and 2D array, respectively. For the 2D array (Fig. 4b), there is a small recirculation in front of the building while such recirculation is absent for the 3D array. Another difference is the areas occupied for the upward and downward motions in the cavities. For the 2D array (Fig.4b), the upward and downward motion appear symmetric, while for the 3D array downward motion occupies the area larger than that for the upward motion. These features are in good agreement with the observations reported in Brown et al. (2001).

5. SUMMARY

A three-dimensional atmospheric prediction model, HOTMAC, was improved so that air flows not only in complex terrain, but also around buildings were simulated. We adopted HSMAC for the non-hydrostatic pressure computation because the method is simple yet efficient. HSMAC is equivalent to solving a Poisson equation, which is commonly used in non-hydrostatic atmospheric models. We tested both HSMAC and solving a Poisson equation, and found that HSMAC produced the results that appear to be more realistic.

The improved HOTMAC was used to simulate air flows over two- and three- dimensional hills and buildings. The modeled results are qualitatively in good agreement with wind tunnel measurements.

There were significant differences between the 2D and 3D block arrays. For example, reattachment distance behind a bluff body was approximately 1 H and 3.5 H for the 3D and 2D arrays, respectively. A small recirculation area formed in front of the 2D block, but not for the 3D block. There was streamline reattachment behind a 2D hill but not for a 3D hill.

We found that the modeled results were sensitive to the inflow boundary conditions. For example, the recirculation area in front of the 2D block array disappeared and the reattachment distance varied when the boundary conditions changed. This might explain why the reattachment distance vary in different wind tunnel experiments.

Reattachment distance increased as the width/height (W/H) ratio increased. Reattachment distances were 2.5H, 3.5H, and 5.5H for W/H = 2H, 4H, and 10H respectively (Snyder and Lawson, 1994). However, reattachment distance for the 2D block array was 3.5H for W/H = 25 (Brown et al., 2001).

Future work includes further refinement of grid spacing from a few meters to a few centimeters. With a smaller grid spacing modeled turbulence will be directly compared with wind tunnel measurements.

REFERENCES

Brown, M.J., Lawson, R.E., DeCroix, D., and Lee R.L., 2001: Comparison of Centerline Velocity Measurements Obtained Around 2D and 3D Building Arrays in a Wind Tunnel. *Proceedings of the 2001 Internatinal Symposium on Environmental Hydraulic, Tempe, AZ, December 2001.*

Hirt, C.W., and Cox, J. L., 1972: Calculating Three-Dimensional Flows around Structures and over Rough Terrain. *J. of Computational Phys*., **10**, 324-340.

Hunt, J.C. R., and Snyder, W. H., 1980: Experiments on stably and neutrally stratified flow over a model three-dimensional hill. *J. Fluid Mech* .,**96**, (4) 671-704.

Ishihara, T., Fujino, Y., and Hibi, K., 2001: A wind tunnel study of separated flow over a two-dimensional ridge and a circular hill. *J. of Wind Engineering,* **89**, 573 – 576. (in Japanese).

Ishihara, T., and Hibi, K., 2000: Numerical Simulation of Turbulent Flow Over a Steep Hill. *J. of Wind Engineering*, **83**, 175-188 (in Japanese).

Kao, C.-Y. J., and Yamada, T., 1988: Use of the CAPTEX Data for Evaluation of a Long-Range Transport Numerical Model with a Four-Dimensional Data Assimilation Technique. *Monthly Weather Review*, **116**, 293-206.

Mellor, G. L., and Yamada T., 1974: A Hierarchy of Turbulence Closure Models for Planetary Boundary Layers. *J. of Atmos. Sci*. **31**, 1791-1806.

Mellor, G. L., and Yamada T., 1982: Development of a Turbulence Closure Model for Geophysical Fluid Problems. *Rev. Geophys. Space Phys*. **20**, 851-875.

Murakami, S., 2000: Computational Environment Design for Indoor and Outdoor Climate, University of Tokyo Press, Tokyo, Japan, 443 (in Japanese).

Snyder, W. H., and Lawson Jr., R. E., 1994: Wind-tunnel study of concentration fields in the vicinity of buildings, 8th Joint Conference on the Applications of Air Pollution Meteorology with the A&WMA, 244-250.

Yamada, T., 1975: The Critical Richardson Number and the Ratio of the Eddy Transport Coefficients Obtained from a Turbulence Closure Model. *J. of Atmos. Sci*. **32**, 926-933.

Yamada, T., 1983. Simulations of Nocturnal Drainage Flows by a q^2l Turbulence Closure Model. *J. of Atmos. Sci.* **40**, 91-106.

Yamada, T., and Bunker S., 1988: Development of a Nested Grid, Second Moment Turbulence Closure Model and Application to the 1982 ASCOT Brush Creek Data Simulation. *J. of Appl. Meteo*. **27**, 562-578.

Yamada, T., and S., Bunker, 1989: A numerical model study of nocturnal drainage flows with strong wind and temperature gradients. *J. of Appl. Meteor.*, **28**, 545-554.